J. Fluid Mech. (1987), *vol.* 179, *pp.* 531–545
Printed in Great Britain

Capillary instability of an annular liquid jet

By J. MEYER AND D. WEIHS

Department of Aeronautical Engineering, Technion – Israel Institute of Technology, Haifa 32000, Israel

(Received 21 May 1986 and in revised form 28 October 1986)

An analytical investigation of the stability of a viscous, annular liquid jet moving in an inviscid medium is presented. This problem is a generalization of the well-known cases of a round cylindrical jet (obtained here when the ratio of internal to external radii tends to zero) and the flat thin liquid sheet (when the ratio above tends to unity). A critical 'penetration' thickness T is defined. When the annulus thickness is greater than T, the annular jet behaves like a full liquid jet; the only unstable perturbations are axisymmetric, and their growth rate is independent of thickness. When the annulus thickness is less than T, the jet behaves like a two-dimensional liquid sheet; the most unstable perturbations are antisymmetric and their growth rate increases as the jet thickness decreases. Therefore, an annular liquid jet with a sufficiently small ring thickness will disintegrate into spherical shells much faster than a full liquid jet disintegrates into drops, in accordance with existing experimental data. Non-dimensional expressions for the penetration thickness are given for both viscous and inviscid jets.

1. Introduction

Much work has been done in recent years on the dynamics of annular liquid jets, because of various applications of such jets in the formation of spherical shells (Kendall 1981), acoustic barriers (Walker & East 1984) and spray guns, among others.

The shape of annular jets, and the related water bells and compound jets, has been extensively studied, including the effects of gravity, surface tension, buoyancy and pressure (or velocity) differences between the inner and outer gas regions (Binnie & Squire 1941; Lance & Perry 1953; Tuck 1982; Gardner & Lloyd 1984; Sanz & Meseguer 1985).

The stability of the annular liquid jet is of interest also from a more general theoretical point of view, as it can be regarded as a general case including, as limits, two well-known situations: (i) that of the circular liquid jet or a cylindrical cavity in a liquid medium and (ii) the thin planar liquid sheet.

These two limiting cases have been extensively investigated during the last century, starting with Rayleigh's (1894) classical analysis of varicose instability of a round jet. The dominant mode of instability leading to breakup was found to be axisymmetric disturbances leading to drop formation. Recent nonlinear studies show this to be still the case (including satellite droplets, etc.) for larger perturbations (Bogy 1979). The effects of velocity (Weber 1931) and viscosity (Sterling & Sleicher 1975) only modify this behaviour quantitatively.

The capillary instability of thin liquid sheets was first studied by Squire (1953) and Hagerty & Shea (1955). Here, instability and breakup are caused by growth of sinuous waves, i.e. including sideways deflections of the centreline. Again various

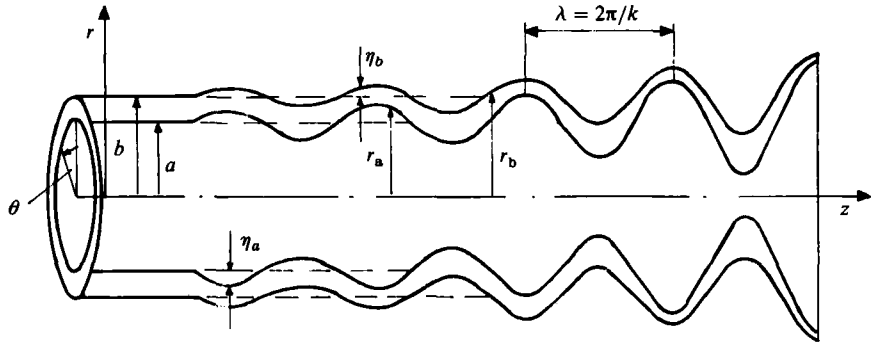

FIGURE 1. Schematic description of an unstable perturbation in an annular jet.

generalizations such as the inclusion of viscosity (Dombrowski & Johns 1963) or spreading (Weihs 1978) did not change the qualitative behaviour.

The annular jet is thus useful in showing how the different dominant modes of instability arise and change in importance as one changes the ratio of inner to outer radii of the annulus from the circular jet limit ($a/b \to 0$) to the ($a/b \to 1$) thin flat sheet case.

In the present paper we examine the linear stability of an infinitely long annular jet moving relative to the media external and internal to the jet. The stability of jet shape to temporal perturbations in the radius is studied, as there is no experimental evidence for the existence of the primary modes of spatial instability discussed by Keller, Rubinow & Tu (1973). A parametric study of the effects of surface tension, viscosity and relative velocity is performed.

2. Formulation of the stability problem

Consider an infinitely long liquid jet of annular cross-section with internal radius a, external radius b, and constant density ρ, viscosity μ and surface tension σ (see figure 1). The jet is moving at fixed axial velocity U through an inviscid medium of constant density $\hat{\rho}(\hat{\rho} \ll \rho)$.

The linear stability of this jet, when subjected to infinitesimal perturbations, will now be studied. Defining (figure 1) a cylindrical coordinate system (r, θ, z) in which the z-axis coincides with the jet axis and moves with it at speed U, one can write the perturbed form of the cylinder, assuming only axisymmetric perturbations, as

$$r_b(z,t) = b + \eta_b(z,t); \quad r_a(z,t) = a + \eta_a(z,t), \tag{1}$$

where $\eta_a, \eta_b \ll a, b$, respectively. The perturbations take the form

$$\eta_j(z,t) = \mathrm{Re}\,(\eta_{0j} \exp(\beta_j t + \mathrm{i} k_j z)) \quad (j = a, b), \tag{2}$$

where β_j are the complex frequencies and k_j the wavenumbers of the perturbations. Conservation of mass over a finite but arbitrary length of the jet much larger than the wavelength leads to the relations (Meyer 1983)

$$\beta_a = \beta_b = \beta; \quad k_a = k_b = k; \quad \frac{\eta_{0b}}{\eta_{0a}} = \frac{a}{b}, \tag{3}$$

when a/b is of order 1. This does not include the limiting case of a full cylinder ($a \to 0$) or a hollow jet (a finite, $b \to \infty$), but these cases do not require the compatibility

conditions (3) as only one characteristic equation is solved. Figures 3, 4, 5, 7 and 8 show that results tending to those for a full jet are obtained when $a/b \geqslant 0.6$, so that the restriction of $a/b = O(1)$ does not cause any practical (or numerical) difficulties.

The equations of motion for the jet and surroundings are obtained by assuming all fluids to be isothermal and incompressible, and neglecting body forces and the viscosity of the surrounding low-density media. The coefficients of surface tension and viscosity of the jet fluid are assumed constant. The axial velocity and pressure are assumed to be independent of the radial coordinate. Perturbing the jet boundaries induces changes in the pressure and velocities both of the jet and its surroundings. One can write the equations of motion for the perturbed quantities $\bar{u}, p$ in the annulus, and $\bar{u}_a, p_a$ and $\bar{u}_b, p_b$ for the media internal to, and outside of the jet, respectively, retaining only first-order terms in the perturbations, as

$$\nabla \cdot \bar{u} = 0; \quad \nabla \cdot \bar{u}_j = 0 \quad (j = a, b), \tag{4}$$

$$\frac{\partial \bar{u}}{\partial t} = -\frac{1}{\rho}\nabla p + \frac{\mu}{\rho}\nabla^2 \bar{u}, \quad \text{(jet)} \tag{5a}$$

$$\frac{\partial \bar{u}_b}{\partial t} + U\frac{\partial \bar{u}_b}{\partial z} = -\frac{1}{\hat{\rho}}\nabla p_b \quad \text{(external medium)}, \tag{5b}$$

$$\frac{\partial \bar{u}_a}{\partial t} + U\frac{\partial \bar{u}_a}{\partial z} = -\frac{1}{\hat{\rho}}\nabla p_a \quad \text{(internal medium)}, \tag{5c}$$

since both the fluid external to, and inside the jet are non-moving (i.e. moving at speed U relative to the jet). The boundary conditions for these equations are taken to hold at the unperturbed radii a and b, again as a result of the small-disturbance model (Squire 1953). These are

no fluid flux through the boundaries

$$u_r = \frac{\partial \eta_j}{\partial t} \quad (j = a, b) \quad \text{at } r = a, b \text{ respectively} \tag{6}$$

for the jet material, and

$$u_{rj} = \frac{\partial \eta_j}{\partial t} + U\frac{\partial \eta_j}{\partial z} \quad \text{at } r = a, b \text{ respectively} \tag{7}$$

for the surrounding media.

The shear stress in the jet vanishes on the boundaries following Sterling & Sleicher (1975):

$$\frac{\partial u_z}{\partial r} + \frac{\partial u_r}{\partial z} = 0 \quad \text{at } r = a, \quad r = b, \tag{8}$$

The normal stress is continuous over the interfaces. The pressure jump due to capillary forces at the interfaces is (on $r = b$ for example) (Levich 1962)

$$p_\sigma = \frac{\sigma}{b} - \frac{\sigma}{b^2}\left(\eta_b + b^2\frac{\partial^2 \eta_b}{\partial z^2}\right). \tag{9}$$

The pressure at the interfaces is, applying (2),

$$-p + 2\mu\frac{\partial u_r}{\partial r} = -p_b + \frac{\sigma}{b^2}(1 - k^2b^2)\,\eta_b \quad \text{at } r = b \tag{10a}$$

and

$$-p + 2\mu\frac{\partial u_r}{\partial r} = -p_a - \frac{\sigma}{a^2}(1 - k^2b^2)\,\eta_a \quad \text{at } r = a \tag{10b}$$

The equations of motion (5) are now expressed by means of potential functions in the inviscid media surrounding the jet, and the velocity in the viscous jet is taken to be the sum of a potential part that fulfils Laplace's equation, and a viscous part described by a stream function (Levich 1962; Sterling & Sleicher 1975). These functions are now assumed, as a result of the form of the perturbations (2), to take the general form

$$F(r,z,t) = f(r)\exp(\beta t + \mathrm{i}kz), \tag{11}$$

where F will be each of the three potential functions, and the stream function. The functions $f(r)$ for the potential and stream functions in the jet and the two surrounding media are of the modified-Bessel-function form, with argument kr for the potentials, and $(k^2+\beta\rho/\mu)^{\frac{1}{2}}$ for the stream function.

After some rather tedious algebraical manipulations,† which follow closely the analysis of Sterling & Sleicher (1975), we obtain the pressure conditions (10a, b) in non-dimensional form, as characteristic equations relating ω – the non-dimensional temporal growth rate ($\omega_b = \beta b/U$ and $\omega_a = \beta a/U$) of a disturbance – to the normalized wavenumbers $\gamma_b = kb$ and $\gamma_a = ka = (a/b)\gamma_b$:

$$\omega_b^2\left(P + D\frac{K_0(\gamma_b)}{K_1(\gamma_b)}\right) + 2\omega_b\left(\mathrm{i}D\gamma_b\frac{K_0(\gamma_b)}{K_1(\gamma_b)} + \frac{\gamma_b}{R_b}\left(2\gamma_b P - 1 + \frac{2\gamma_b^2}{\gamma_{1b}^2-\gamma_b^2}(\gamma_b P - \gamma_{1b}P_1)\right)\right) = \frac{1}{W_b}\left((1-\gamma_b^2)\gamma_b + DW_b\gamma_b^2\frac{K_0(\gamma_b)}{K_1(\gamma_b)}\right), \tag{12}$$

where $D = \hat{\rho}/\rho$, $R_b = \rho U b/\mu$, $W_b = \rho U^2 b/\sigma$, K_0, K_1, I_0, I_1 are modified Bessel functions,

$$P = \frac{1/\gamma_a - (K_1(\gamma_a)I_0(\gamma_b) + I_1(\gamma_a)K_0(\gamma_b))}{K_1(\gamma_b)I_1(\gamma_a) - K_1(\gamma_a)I_1(\gamma_b)}, \tag{13a}$$

$$P_1 = \frac{1/\gamma_{1a} - (K_1(\gamma_{1a})I_0(\gamma_{1b}) + I_1(\gamma_{1a})K_0(\gamma_{1b}))}{K_1(\gamma_{1b})I_1(\gamma_{1a}) - K_1(\gamma_{1a})I_1(\gamma_{1b})}, \tag{13b}$$

$$\gamma_{1a} = \left(k^2 + \beta\frac{\rho}{\mu}a\right)^{\frac{1}{2}}; \quad \gamma_{1b} = \left(k^2 + \beta\frac{\rho}{\mu}b\right)^{\frac{1}{2}}$$

and

$$\omega_a^2\left(Q - D\frac{I_0(\gamma_a)}{I_1(\gamma_a)}\right) + 2\omega_a\left(-\mathrm{i}D\gamma_a\frac{I_0(\gamma_a)}{I_1(\gamma_a)} + \frac{\gamma_a}{R_a}\left(2\gamma_a Q - 1 + \frac{2\gamma_a^2}{\gamma_{1a}^2-\gamma_a^2}(\gamma_a Q - \gamma_{1a}Q_1)\right)\right) = -\frac{1}{W_a}\left((1-\gamma_a^2)\gamma_a + DW_a\gamma_a^2\frac{I_0(\gamma_a)}{I_1(\gamma_a)}\right), \tag{14}$$

with Reynolds and Weber numbers $R_a = \rho U a/\mu$ and $W_a = \rho U^2 a/\sigma$, respectively,

$$Q(\gamma_b,\gamma_a) = P(\gamma_a,\gamma_b) = \frac{1/\gamma_b - (K_1(\gamma_b)I_0(\gamma_a) + I_1(\gamma_b)K_0(\gamma_a))}{K_1(\gamma_a)I_1(\gamma_b) - K_1(\gamma_b)I_1(\gamma_a)} \tag{15}$$

and

$$Q_1(\gamma_{1b},\gamma_{1a}) = P_1(\gamma_{1a},\gamma_{1b})$$

in similar fashion.

Equations (12) and (14) are thus the characteristic equations to be solved with instability occurring when $\omega_j > 0$ for a given γ_j. The compatibility conditions (3)

† Details of which are available, upon request, from the authors.

allow for only one of these to be solved for annular cases where $a/b = O(1)$. These equations are of the form

$$\omega_j = \omega_j\left(\gamma_j, D, \frac{a}{b}, R_j, W_j\right) \quad (j = a, b) \tag{16}$$

and thus, for $D, a/b, R_j, W_j$ known, ω_j is only a function of γ_j. The terms including P_1, Q_1 introduce an implicit dependence on ω, so that (12) and (14) are not simple quadratic dependences, for viscous jets. For inviscid jets, $R_a = R_b \to \infty$ and these terms vanish.

The solutions of (12) and (14) enable the determination of unstable perturbations, and specifically, finding the wavenumber γ^* that has the maximum growth rate (ω^*) in the linear regime. This is usually (Sanz & Meseguer 1985) taken to be the wavenumber of the disturbance that finally causes breakup of the jet. We do not expect the twin maxima observed for compound jets with differing surface-tension coefficients at the inner and outer radius. We essentially have a case of equal surface-tension coefficients but negligible inner jet density for which (Sanz & Meseguer 1985) only one maximum is obtained.

3. Analytical solutions

Equations (12) and (14) are the general characteristic equations for studying the stability of the annular jet. No general analytical solution is possible owing to the appearance of the growth rate in the viscous term (in γ). However, the neutral stability limit can be approximately obtained analytically in closed form, and can serve as a partial check on the equations. Also, the limits of the full jet and thin flat sheet will be retrieved. In the latter two examples, the requirement of $a/b = O(1)$ is not fulfilled, but on the other hand only one characteristic equation is required, so this restriction is not relevant.

3.1. *Wavenumber for neutral stability*

The external characteristic equation is of the form

$$G_1 \omega_b^2 + 2\omega_b(\mathrm{i}G_2 + G_3) = G_4 \tag{17}$$

and the difficulty precluding a closed-form solution appears in the coefficient G_3. The wavenumber of neutral stability has (by definition) $\omega = 0$, so that for this wavenumber

$$G_4 = 0, \tag{18}$$

i.e. (18) can serve as the relation between the various parameters resulting in neutral stability. From (12)

$$(1-\gamma_b^2)\gamma_b + DW_b\gamma_b^2\frac{K_0(\gamma_b)}{K_1(\gamma_b)} = 0, \tag{19}$$

with a similar equation for the inner boundary, as a function of γ_a. $K_0(z)/K_1(z) < 1$ for all finite values of z, and D is $O(10^{-3})$ for a typical liquid in air, so that for $W_b \approx O(1)$ the wavenumber of neutral stability obtained from the external equation $(\gamma_0)_b$ is

$$(\gamma_0)_b \approx 1, \tag{20}$$

and when $W_b = 0$ as in Rayleigh's (1894) case of no external fluid, $(\gamma_0)_b = 1$, as originally obtained by Rayleigh.

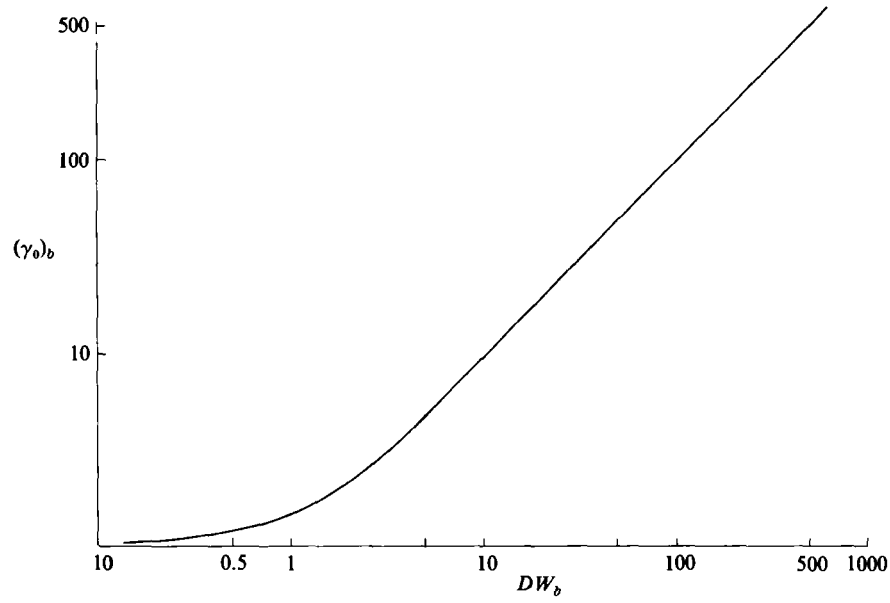

FIGURE 2. Dependence of the wavenumber of neutral stability on Weber number.

Another limit enabling an approximate analytical solution is that of very fast relative motion (still within the incompressible regime), i.e. $W_b \gg 1$. For example, a water jet of 1 cm external radius moving at 50 m/s in air at 20 °C has $W_b \approx 3.5 \times 10^5$. Equation (19) then leads, using the expressions for large arguments of the Bessel functions, to

$$(\gamma_0)_b \approx W_j D \quad (j = a, b) \tag{21}$$

or, in dimensional quantities,

$$(k_0)_b \approx (k_0)_a \approx \frac{\hat{\rho} U^2}{\sigma}, \tag{22}$$

i.e. for large enough values of the Weber number the wavenumber of neutral temporal stability k_0 obtained from either (12) or (14) is identical with that obtained first by Weber (1931) for the round full jet, and by Squire (1953) for the flat thin liquid sheet. Figure 2 shows the variation of $(\gamma_0)_b$ with $W_b D$, from which one can see that

$$(\gamma_0)_b = O(DW_b)$$

or

$$k_0 = O\left(\frac{\hat{\rho} U^2}{\sigma}\right) \tag{23}$$

for most cases of practical interest, when $DW \geqslant 1$.

3.2. *A full liquid jet* ($a \to 0$)

The most complete analytical investigation of a viscous liquid jet in a gas medium appears in Sterling & Sleicher (1975). The present external characteristic equation (12) differs from their equation by including expressions P and P_1 instead of their $I_0(\gamma_b)/I_1(\gamma_b)$ and $I_0(\gamma_{1b})/I_1(\gamma_{1b})$ respectively. The internal equation (14) is obviously not relevant here.

When $a \to 0$, for $DW_b \gg 1$, which results in $\gamma_b \gg 1$, and using asymptotic expressions for Bessel functions, we obtain

$$P \to \frac{I_0(\gamma_b)}{I_1(\gamma_b)}; \quad P_1 \to \frac{I_0(\gamma_{1b})}{I_1(\gamma_{1b})}, \tag{24}$$

i.e. the external characteristic equation tends to the equation for a full liquid jet, retrieving existing solutions.

3.3. *A gas jet moving in a liquid medium* ($b \to \infty$)

This case was first analysed by Rayleigh (1894) and more recently by Chandrasekhar (1961), limited to quiescent inviscid cylinders in a vacuum. Here the external equation (12) is not relevant.

When $b \to \infty$, and by use of asymptotic relations, expressions Q and Q_1 in the internal characteristic equation (14) become

$$Q \to -\frac{K_0(\gamma_a)}{K_1(\gamma_a)}; \quad Q_1 \to -\frac{K_0(\gamma_{1a})}{K_1(\gamma_{1a})}. \tag{25}$$

No comparison being available for the general case, we take the Rayleigh case $\hat{\rho} = \mu = U = 0$, and (14) with (25) reduces to

$$\omega_a^2 = \frac{1}{W_a}(1-\gamma_a^2)\,\gamma_a \frac{K_1(\gamma_a)}{K_0(\gamma_a)}, \tag{26}$$

which is identical with the equation given by Chandrasekhar (1961). Solution of this equation for the dominant wavelength λ^* is

$$\lambda^* = 12.98a \tag{27}$$

as given by Rayleigh (1894).

3.4. *A thin liquid sheet* ($a/b \to 1$)

A third limiting case for the annular liquid jet is obtained when the ratio of radii tends to unity ($a/b \to 1$). This case represents a thin liquid sheet as curvature effects vanish. Stability of sheets was first analysed by Squire (1953) for an inviscid liquid, followed by Dombrowski & Johns (1963), who included viscous effects.

Assuming that $DW_b \gg 1$, $DW_a \gg 1$, one can write P (equation (13a)) approximately by using asymptotic expressions for the Bessel functions. Now, we assume $(\gamma_b - \gamma_a) < 1$, which is equivalent to $(b-a) \ll b$, thus obtaining a thin liquid jet. The expression for P reduces to

$$P \approx \tfrac{1}{2}(\gamma_b - \gamma_a). \tag{28}$$

Now, defining the jet thickness as $2h = b-a$ and its corresponding non-dimensional values by

$$\omega_h = \beta\frac{h}{u} = \omega_{h\mathrm{R}} + \mathrm{i}\omega_{h\mathrm{I}}; \quad \gamma_h = kh = \tfrac{1}{2}(\gamma_b - \gamma_a);$$

$$W_h = \rho\frac{U^2 h}{\sigma}; \quad R_h = \rho\frac{Uh}{\mu},$$

the external characteristic equation (12) reduces to

$$\omega_h^2\{\gamma_h + D\} + 2\omega_h\left\{\mathrm{i}D\gamma_h - \frac{h\gamma_h}{bR_h}\right\} = \frac{1}{W_h}\{-\gamma_h^3 + DW_h\,\gamma_h^2\}. \tag{29}$$

Let us first analyse the inviscid case ($R_h \gg 1$) to compare this equation with Squire's (1953) analysis. Also, we again take $D \ll 1$. The characteristic equation is then

$$\omega_h^2 + 2\mathrm{i}D\omega_h = \frac{1}{W_h}(-\gamma_h^2 + DW_h\gamma_h), \tag{30}$$

with solution

$$\omega_h \approx -\mathrm{i}D \pm \left(\frac{1}{W_h}(-\gamma_h^2 + DW_h\gamma_h)\right)^{\frac{1}{2}}. \tag{31}$$

For an unstable jet, $\omega_{h\mathrm{R}} > 0$, and so the limiting wavenumber is still

$$\gamma_{h0} = DW_h = \hat{\rho}\frac{U^2 h}{\sigma}. \tag{32}$$

The maximum growth rate $\omega_{h\mathrm{R}}^*$ is obtained for

$$\gamma_h^* \approx \tfrac{1}{2}DW_h = \tfrac{1}{2}\gamma_{h0} = \tfrac{1}{2}\hat{\rho}\frac{U^2 h}{\sigma}, \tag{33}$$

and its value is

$$\omega_{h\mathrm{R}}^* = \beta_{\mathrm{R}}^*\frac{h}{U} = \frac{1}{2}\left(\frac{\hat{\rho}}{\rho}DW_h\right)^{\frac{1}{2}} = \hat{\rho}_2^{\frac{1}{2}}U\left(\frac{h}{\rho\sigma}\right)^{\frac{1}{2}}. \tag{34}$$

These three quantities are identical with those obtained by Squire (1953).

The characteristic equation (30) holds also in the viscous case, under the conditions $\gamma_b \gg 1, 2\gamma_h < 1$, because in that case R_b^{-2} is small compared with the right-hand side of (29). (One has $O(10^{-6}$–$10^{-10})$ compared with $O(10^{-4})$.) This result is in agreement with a study by Dombrowski & Johns (1963) for a viscous liquid sheet, which shows that in our case the results for the viscous fluid reduce to the inviscid solution.

Finally, the internal characteristic equation (14), under the same conditions and by taking similar limits reduces to (30), just like the external equation.

The condition $(\gamma_b - \gamma_a) = 2\gamma_h < 1$ implies the existence of a 'penetration thickness' T_{c}, defined by

$$DW_h = 0.5 \quad \text{or } T_{\mathrm{c}} = \left(\hat{\rho}\frac{U^2}{\sigma}\right)^{-1}, \tag{35}$$

since the wavenumber of neutral stability is $\gamma_{h0} = DW_h = \hat{\rho}U^2 h/\sigma$. Thus an annular liquid jet whose ring thickness is less than T_{c} behaves like a thin inviscid liquid sheet, as will be discussed later.

4. Results and discussion

4.1. *Maximum growth rate ω_{R}^* and dominant wavenumber γ^**

The full characteristic equations are now solved numerically and results, especially that of the maximum growth rate ω_{R}^* and dominant wavenumber γ^*, are presented here, and shown in figures 3–8.

These dominant values are presented in a normalized form:

$$\bar{\omega}_{\mathrm{R}}^* = \frac{\omega_{\mathrm{R}}^*}{R_b} = \frac{\omega_{h\mathrm{R}}^*}{R_h} = \frac{\beta_{\mathrm{R}}^*}{(\rho U^2/\mu)}, \tag{36}$$

$$\bar{\gamma}^* \frac{\gamma^*}{DW_b} = \frac{k^*}{(\hat{\rho}U^2/\sigma)}. \tag{37}$$

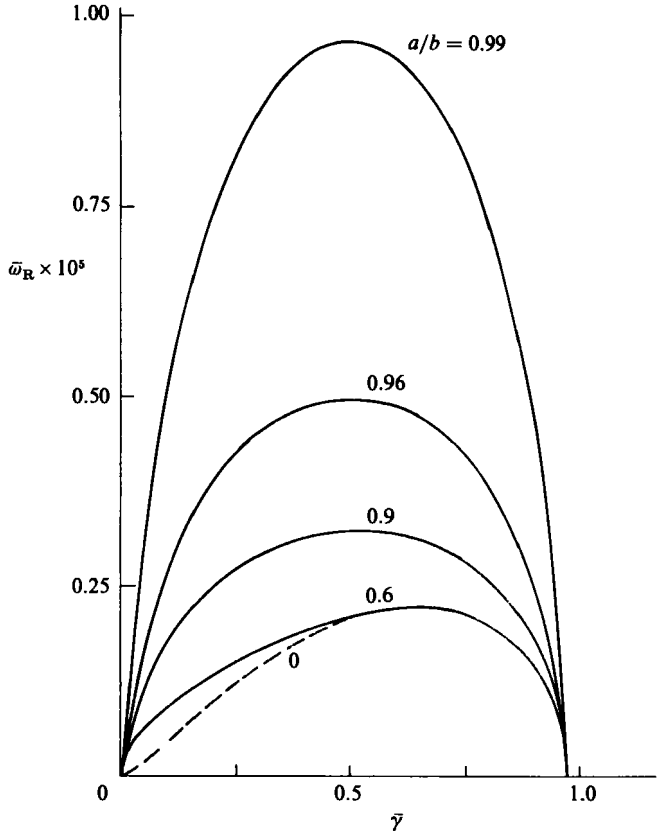

FIGURE 3. Dependence of non-dimensional disturbance growth rate $\bar{\omega}_R$ on wavenumber $\bar{\gamma}$, for various ratios of diameters. The broken line shows the full-jet case.

This form of non-dimensionalization was found to be useful (Meyer 1983) in that the quantities $\bar{\omega}^*$ and $\bar{\gamma}_R^*$ are dependent only on a single material parameter, the ratio of capillary to viscosity forces:

$$N_b = \frac{DW_b}{R_b} = \hat{\rho}\frac{U\mu}{\rho\sigma}. \tag{38}$$

As found in the full-liquid-jet case, viscous effects are small for $N_b < 10^{-2}$, so results will be shown for one inviscid ($N_b < 10^{-2}$) and one viscous liquid ($N_b > 10^{-2}$).

The first case presented is an annular water jet ($\mu = 0.01$ P; $\sigma = 70$ dyne/cm) of radius $b = 1$ cm, moving at the velocity $U = 1000$ cm/s in air ($\hat{\rho}/\rho = 1/800$). Corresponding non-dimensional ratios are Weber number $DW_b = 17.9$, Reynolds number $R_b = 10^5$ and their ratio $N_b = 1.8 \times 10^{-4}$.

Figure 3 shows the variation of $\bar{\omega}_R$ with the wavenumber $\bar{\gamma}$ for different ratios a/b. Figures 4 and 5 show the dependence of $\bar{\gamma}^*$ and $\bar{\omega}_R^*$ on the ratio a/b (or the thickness $2h/b$). Also shown are results for the same water jet but with radius $b = 100$ cm, showing the effects of changing radius (and W_b), and at the velocity $U = 10000$ cm/s, showing effects of velocity. In both cases, at the limit $a/b \to 0$, $\bar{\gamma}^*$ and $\bar{\omega}_R$ correspond to the values of the liquid jet (Meyer 1983), for here $DW_b \gg 1$.

Values of $\bar{\gamma}^*$ and $\bar{\omega}_R^*$ do not change significantly as a/b increases to near the

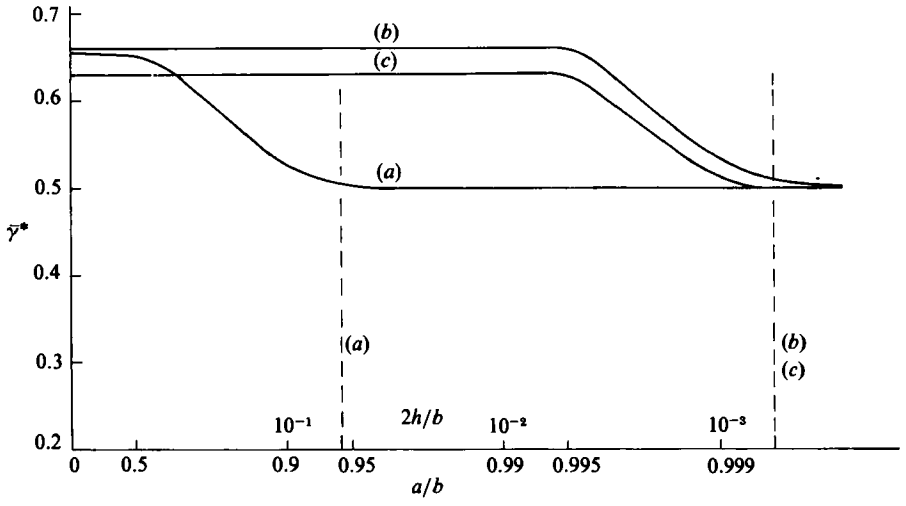

FIGURE 4. The non-dimensional wavenumber of maximum instability $\bar{\gamma}^*$ (dominant wavenumber) versus the ratio a/b, for annular water jets. The broken lines indicate the capillary penetration thickness in each case.

	U (cm/s)	b (cm)	DW_b	R_b	N_b
(*a*)	1000	1	17.9	10^5	1.8×10^{-4}
(*b*)	1000	100	1786.0	10^7	1.8×10^{-4}
(*c*)	10000	1	1786.0	10^6	1.8×10^{-3}

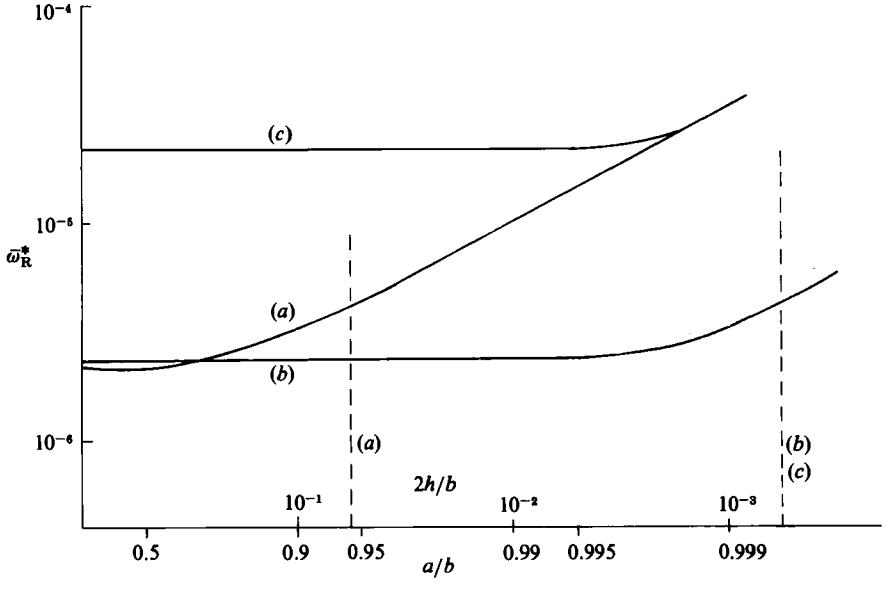

FIGURE 5. Maximum growth rate $\bar{\omega}_R^*$ versus ratio a/b, for various annular water jets. For notation see figure 4.

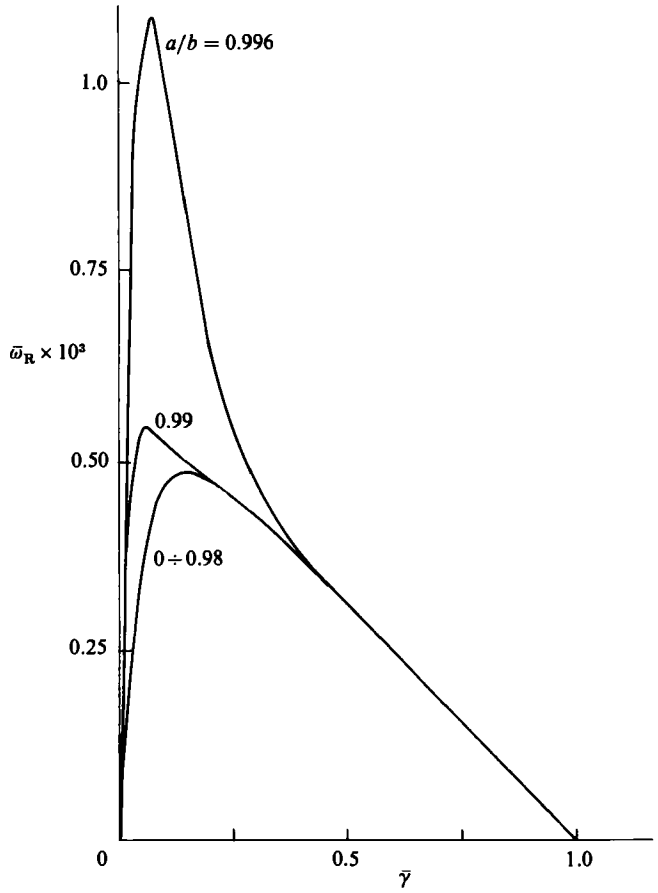

FIGURE 6. Dependence of disturbance growth rate $\bar{\omega}_R$ on wavenumber $\bar{\gamma}$, for annular viscous liquid jets of various ratios of diameters $DW_b = 4167$; $R_b = 10000$; $N_b = 0.42$.

penetration thickness T_c (defined by (35) and specified in the figures), where there is a sharp change in their values: $\bar{\gamma}^*$ decreases to the value of the liquid sheet (0.50) given by Squire (1953) and (33), while $\bar{\omega}_R^*$ increases with thickness decrease (as from (34)). Within the limits of the penetration thickness, values of $\bar{\omega}_R^*$ are in good agreement with values obtained by Dombrowski & Johns (1963).

The criterion for the penetration thickness corresponds to a sharp change in characteristic behaviour of the annular jet from a jet-like instability to a sheet-like instability. In particular, below the penetration thickness the growth rate $\bar{\omega}_R^*$ increases considerably, up to an order of magnitude or more, faster than the growth rate of the full jet, and consequently breakup time and length decrease considerably.

The other cases presented in figures 4 and 5 confirm the previous arguments about a penetration thickness that depends only on W_h (or W_b), and corresponds to a change in the behaviour of the annular jet. In particular, this thickness T_c is independent of the radius b. On the other hand, the characteristic values $\bar{\gamma}^*$ and $\bar{\omega}_R^*$ for small a/b ratio, and at the limit $a/b \to 0$, depend on the ratio N_b, as shown by Meyer (1983).

Next, we examine an annular viscous liquid jet ($\mu = 1$ P; $\sigma = 30$ dyne/cm), with a radius $b = 1$ cm, and at the velocity $U = 10000$ cm/s. Corresponding non-dimensional ratios are $DW_b = 4167$, $R_b = 10^4$ and $N_b = 0.42$.

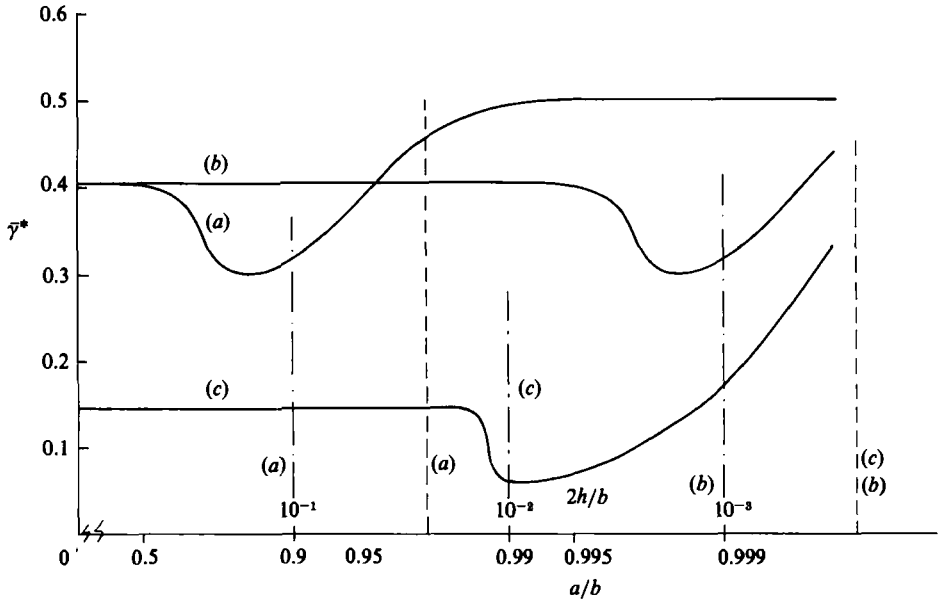

FIGURE 7. Dominant wavenumber $\bar{\gamma}^*$ versus ratio a/b, for annular viscous liquid jets with $\mu = 1$ P, $\sigma = 30$ dyne/cm. ----, capillary penetration thickness; —·—, viscous penetration thickness.

	U (cm/s)	b (cm)	DW_b	R_b	N_b
(a)	1000	1	41.7	10^3	0.042
(b)	1000	100	4167.0	10^5	0.042
(c)	10000	1	4167.0	10^4	0.42

Figure 6 shows the variation of $\bar{\omega}_R$ with the wavenumber $\bar{\gamma}$ for different ratios a/b. In comparison with the inviscid case (figure 3), it is shown that the curve of $\bar{\omega}_R$ has its maximum at a lower value of $\bar{\gamma}$, and that it remains constant up to higher values of the ratio a/b. Figures 7 and 8 show dependence of $\bar{\gamma}^*$ and $\bar{\omega}_R^*$ on the ratio a/b. Results are also shown for the same liquid jet with radius $b = 100$ cm ($DW_b = 4167$) and $b = 1$ cm ($DW_b = 41.7$) and axial velocity $U = 1000$ cm/s, to highlight the effect of the non-dimensional parameters N_b and W_b.

Some trends that have appeared in the inviscid cases are still valid for these highly viscous jets: at the limit $a/b \to 0$, $\bar{\gamma}^*$ and $\bar{\omega}_R^*$ correspond to the values of the full liquid jet. Again a penetration thickness T_c exists such that a jet with ring thickness smaller than it behaves like a liquid sheet, retrieving the Squire (1953) and Dombrowski & Johns (1963) results: $\bar{\gamma}^*$ is 0.50, and $\bar{\omega}_R^*$ increases as the annulus becomes thinner. Under this condition viscosity does not change the results for both liquid sheets and annular jets, as previously shown analytically.

But thicker viscous annular jets behave differently. First, for small a/b ratios, $\bar{\gamma}^*$ is smaller than 0.50 (Meyer 1983), and so it has to increase in order to match the value of the liquid sheet. Secondly, before $\bar{\gamma}^*$ increases towards 0.50, at T_c, it first decreases at some characteristic thickness. This thickness may be called a viscous penetration thickness T_v, in contrast to T_c, which will be called the capillary penetration thickness. When $2h < T_v$ the annular viscous jet behaves like a viscous liquid sheet, such as studied by Dombrowski & Johns (1963), and specifically $\bar{\gamma}^* < 0.5$. At $2h < T_c < T_v$ the viscous liquid sheet itself behaves as the inviscid one, and so does

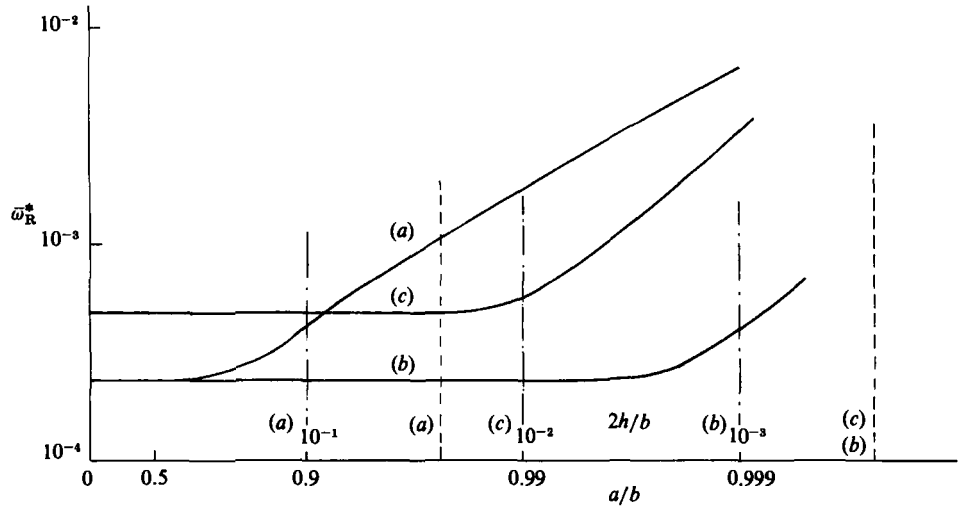

FIGURE 8. Maximum growth rate $\bar{\omega}_R^*$ versus ratio a/b, for an annular viscous liquid jet. For notation see figure 7.

the viscous circular jet. The growth rate $\bar{\omega}_R^*$, in the viscous case, already begins to increase at the viscous thickness T_v. This thickness was not obtained analytically, but on the basis of the numerical results. The viscous penetration thickness can be correlated to the Reynolds number R_h:

$$(R_h)_v = 50 \quad \text{or } T_v = 100\left(\frac{\rho U}{\mu}\right)^{-1}. \tag{39}$$

The different cases shown in figures 7 and 8 confirm the above:
for small a/b ratios, the dominant values $\bar{\gamma}^*$ and $\bar{\omega}_R^*$ depend on N_b;
capillary thickness T_c depends on W_h (W_b);
viscous thickness T_v depends on R_h (or R_b).

4.2. *Penetration thicknesses*

A capillary penetration thickness T_c for annular liquid jets was defined in (35). If the annular jet is thicker than T_c it behaves like a full liquid jet with constant $\bar{\omega}_R^*$. Otherwise, it behaves like a liquid sheet, where the wavenumber of maximal instability $\bar{\omega}_R^*$ grows as the thickness decreases.

For viscous annular liquid jets, there exists also a viscous penetration thickness T_v defined by (39). If the annular jet is thinner than T_v it behaves like a viscous liquid sheet. If the annular jet is thinner than T_c it behaves again like an inviscid liquid sheet. In both cases, $\bar{\omega}_R^*$ grows as the thickness decreases.

This process exists naturally only if $T_v > T_c$; otherwise no effect of viscosity is noted. So, viscous effects are significant when

$$\frac{100h}{R_h} > \frac{h}{DW_h}$$

or

$$\frac{DW_h}{R_h} = \frac{DW_b}{R_b} = N_b > 10^{-2}.$$

This criterion for the significance of effects is the same as the criterion found in the full liquid jet (Meyer 1983), based on an analysis of the order of magnitude of

expressions in the characteristic equation. Also, in the full liquid jet, the value of $N_b = 10^{-2}$ corresponds to a dominant wavenumber $\bar{\gamma}^* = 0.50$, separating inviscid jets ($\bar{\gamma}^* > 0.50$) from viscous jets ($\bar{\gamma}^* < 0.50$).

These thicknesses T_c and T_v were called penetration thicknesses, according to the following model of the capillary instability of an annular jet:

For low ratios of radii a/b, or large thickness ratios $2h/b$, the jet is thick enough that there is no relation between perturbations on the external and the internal radii. The annular jet behaves like a full liquid jet (if $a \to 0$ and b is finite) or like a hollow jet (if a is finite and $b \to \infty$). Unstable perturbations are axisymmetric, and growth rate β_R^* is independent of thickness.

For viscous annular jets, and jet thickness smaller than T_v, perturbations on the external radius penetrate down into the internal radius and vice versa, owing to the diffusion of vorticity by viscosity acting to correlate the flow conditions and perturbations in the liquid.

For both viscous and inviscid annular jets thinner than T_c, again perturbations on the external and internal radii penetrate one into the other, but now owing to the capillary influence acting in a similar manner to the viscosity. For viscous jets the influence of viscosity becomes negligible relative to the capillary or thickness effect. For jets with $N_b < 10^{-2}$ the capillary effect is stronger than the viscous one for all values of the ratio a/b. In those two ranges $2h < T_v$ and $2h < T_c$, perturbations are common to both the internal and external radii. The jet thickness is small enough that the annular jet may be viewed locally as a thin liquid sheet, for which the principal mode of instability is antisymmetric (sinuous). As a result the rate of growth of disturbances is much larger than for thick jets.

This also explains why the condition $DW_b \gg 1$ is required so that the annular jet with $a \to 0$ should behave as a full cylindrical jet. For, if $DW_b \approx 1$, $T_c/b = 1/DW_b \approx 1$, and the penetration thickness is of the same order as the jet radius itself. So, even at the limit $a \to 0$, the annular jet will behave as a liquid sheet, and not as a circular jet.

In contrast, for the case $b \to \infty$, even for small DW_a, a jet thickness $2h = b - a$ larger than T_c will always be reached, and so at the limit $b \to 0$ the annular jet will behave as a hollow jet.

This study was supported by the Technion V.P.R.–L. Kraus Research Fund.

REFERENCES

Baird, M. H. I. & Davidson, J. F. 1962 Annular jets. I. Fluid dynamics. *Chem. Engng Sci.* **17**, 467–472.

Binnie, A. M. & Squire, H. B. 1941 Liquid jets of annular cross section. *Engineer* **171**, 236–238.

Bogy, D. B. 1979 Drop formation in a circular liquid jet. *Ann. Rev. Fluid Mech.* **11**, 207–228.

Chandrasekhar, S. 1961 *Hydrodynamic and Hydromagnetic Stability*, pp. 537–542. Clarendon.

Dombrowski, N. & Johns, W. R. 1963 The aerodynamic instability and disintegration of viscous liquid sheets. *Chem. Engng Sci.* **18**, 203–214.

Gardner, G. C. & Lloyd, T. 1984 Annular buoyant jets. *Intl J. Multiphase Flow* **10**, 635–641.

Hagerty, W. W. & Shea, J. F. 1955 A study of the stability of plane fluid sheets. *Trans. ASME* E: *J. Appl. Mech.* **22**, 509–514.

Keller, J. B., Rubinow, S. I. & Tu, Y. 1973 Spatial instability of a jet. *Phys. Fluids* **16**, 2052–2955.

Kendall, J. M. 1981 Hydrodynamic performance of an annular liquid jet. In *Proc. 2nd Intl Coll. on Drops and Bubbles, Monterey, Ca, JPL Publication* 82–7, pp. 79–87.

LANCE, G. N. & PERRY, R. L. 1953 Water bells. *Proc. Phys. Soc.* B **66**, 1067–1072.

LEVICH, V. G. 1962 *Physicochemical Hydrodynamics*, pp. 372–377, 626–650. Prentice-Hall.

MEYER, J. 1983 Investigation of the instability of an annular hollow jet. M.Sc. thesis, Technion – Israel Institute of Technology, 102 pp.

RAYLEIGH, LORD 1894 *Theory of Sound*, vol. II, 2nd edn, pp. 351–365. Dover.

SANZ, A. & MESEGUER, J. H. 1985 One-dimensional linear analysis of the compound jet. *J. Fluid Mech.* **159**, 55–68.

SQUIRE, H. B. 1953 Investigation of the instability of a moving liquid film. *Brit. J. Appl. Phys.* **4**, 167–169.

STERLING, A. M. & SLEICHER, C. A. 1975 The instability of capillary jets. *J. Fluid Mech.* **68**, 477–495.

TUCK, E. O. 1982 Annular water jets. *IMA J. Appl. Maths* **29**, 45–58.

WALKER, G. & EAST, R. A. 1984 Shock tube studies of a water sheet inertial energy absorber to reduce blast overpressure. In *Proc. Symp. Shock and Blast Wave Phenomena, Cranfield, UK.* Paper C-2, 16 pp.

WEBER, K. 1931 Zum zerfall eines flussigkeitsstrahles. *Z. angew. Math. Mech.* **11**, 136–154.

WEIHS, D. 1978 Stability of thin, radially moving liquid sheets. *J. Fluid Mech.* **87**, 289–298.